Electrical Modeling of Molten Salt Electro-Refining Processes

Alexandre Oury*[1], Patrick Namy[1]
[1]SIMTEC, 8 rue Duployé, 38100 Grenoble, France
*Corresponding author: alexandre.oury@simtecsolution.fr

Abstract: The optimization of the design and of the operating conditions of high-temperature electrolysis cells for the recovery of metals can be done by rather simple electrical simulations. The implementation of both primary and secondary current distribution models applied to an electrolysis cell for the recovery of rare earths is here demonstrated. Comparison between the two approaches are made. The effect of the prescribed current on the reaction rate distribution is also assessed, using the secondary current model.

Keywords: Electrolysis, current distribution, primary current, secondary current, rare earth.

1. Introduction

A common pyrometallurgical route for the recovery of numerous metals and rare earths is high-temperature molten salt electrolysis. This process involves an electrolyte made of a molten salt in which the metal to be recovered, most commonly present in its oxide form, is dissolved. When a current is applied between the cathode and anode, the metal is deposited as a solid or a liquid at the cathode, while some gas (generally a carbon oxide, such as CO or CO_2) evolves at the carbon-based anode, as depicted in figure 1.

Numerical simulation can be advantageously employed to predict the main cell features (e.g., the reaction rate distribution on the electrodes, the cell voltage, or the electrolyte temperature) in order to optimize the design and operational conditions of the process. Even though high-temperature electrolysis involves many physical phenomena that are complex and strongly coupled to one another, the reaction rate distribution on the electrodes can be approximated with a rather simple electrostatic approach that involves the calculation of the current densities associated with the reactions.

In this article, we describe a computational approach for predicting current distributions in a typical molten salt electro-refiner. Two types of current distribution (primary and secondary) are addressed. A simple approach to implement current-predicting models for the cell in COMSOL Multiphysics is presented. The simulated current at the electrodes' surface (the reaction rate) are analyzed, the main differences between the primary and the secondary description are explained and the effect of increasing the applied current is assessed.

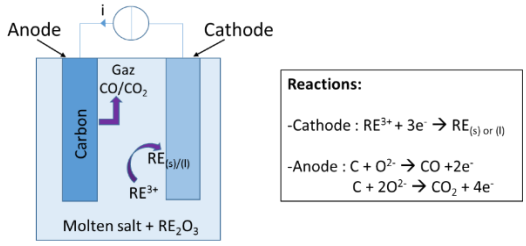

Figure 1. Principle of a molten salt electrolysis cell for the electro-refining of rare earths.

2. Model description

2.1 Geometry

In the small-scale rare earth electro-refiner studied here, the electrodes are made of cylindrical rods partially immersed in the molten salt electrolyte, as shown represented in figure 2. It consists of multiple anode rods (diameter 1.5 cm) regularly arranged in a circle around a central cathode rod (diameter 2 cm). The molten salt-based electrolyte contains the rare earth (for example neodymium) to be recovered at the cathode along with several other elements.

Owing to symmetrical considerations, the computation of only 1/32nd of the geometry (see fig. 2) is sufficient to capture the behavior of the entire reactor, which considerably diminishes the degrees of freedom of the model.

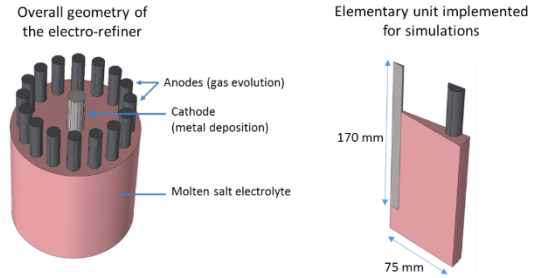

Figure 2. Geometry of the molten salt electro-refiner considered for simulation (left) and elementary unit obtained after consideration of the symmetry planes (right).

2.2. Equations and boundary conditions

The present models only focus on the electrical behavior of the electro-refining cell, i.e. on the current that flows across the system. The latter is considered to be isothermal and no effect of mass transport is accounted for in the electrolyte.

The current flow in an electrochemical device can be described by three different approaches, the so-called primary, secondary, and tertiary distributions. The type of distribution depends on the kinetics of the reactions taking place at the electrodes' surface and whether the cell is limited by the transport of active species. The goal of the present didactic study is to show how the primary and the secondary current approaches can be numerically implemented in Comsol and to highlight the main differences between the two methods in terms of simulated current.

In the primary current distribution, it is assumed that the reaction kinetics are so fast that no overpotential accompanies the activation of the reactions. The cell can be considered as a simple resistive charge conductor. In the secondary current distribution, the activation overpotentials of the reaction(s) at the electrode/electrolyte interfaces are accounted for. This can be required when the electrochemical reactions are significantly slow, which is generally the case for processes involving gas evolution reactions.

The only equation that is solved for in all domains for the two current approaches is the conservation of the current density $\vec{j}$:

$$\nabla.\vec{j} = 0$$

which is written, including the electric potential:

$$\nabla.(-\sigma\vec{\nabla}V) = 0$$

where V is the electric potential and σ the conductivity of the region (electronic in the solid domains and ionic in the electrolyte).

The boundary conditions defined for the two current models are summarized in table 1. The current flow is provided under galvanostatic condition, by applying a normal current density j_{app} at each top surfaces of the anodes while a ground condition is prescribed at the top surface of the cathode to provide a reference value for the potential.

The difference between the two current models lies in the conditions that are prescribed at the electrodes/electrolyte interfaces. For the case of primary current, a continuity condition is defined for the potential on the cathode/electrolyte boundaries and a potential jump is prescribed at the anode/electrode boundaries to take into account the equilibrium Nernst voltage ΔE^0 of the cell (sometimes referred to as the decomposition voltage). In the secondary current model, Butler-Volmer kinetics expressions are set at the electrode/electrolyte interfaces, describing the activation overpotential of each reaction. These relations involve the exchange current density of each electrode reaction ($i_{0,A}$ for the anode and $i_{0,C}$ for the cathode) which reflects the kinetics of the electrochemical process.

The value of the different parameters used as boundary conditions are given in table 2. A high value of $i_{0,C}$ was chosen since the cathodic reduction of metals are generally reversible processes (fast kinetics). On the opposite, $i_{0,A}$ was associated with a much lower value, taking into account that gas evolution reactions need a significant overpotential to be activated.

Table 1. Boundary conditions applied for the primary and the secondary current models.

Boundary	**Conditions in the primary current model**	**Conditions in the secondary current model**
Top anode surfaces	Prescribed normal current density: j_{app}	Prescribed normal current density j_{app}
Top cathode surface	Ground: $V_{cathode} = 0$	Ground: $V_{cathode} = 0$
Anode/electrolyte interfaces	Nernst potential jump: $V_{anode} = V_{electrolyte} + \Delta E^0$	Butler-Volmer kinetics: $\vec{j}.\vec{n} = i_{0,A}(e^{\frac{0,5F}{RT}\eta_A} - e^{-\frac{0,5F}{RT}\eta_A})$ with $\eta_A = V_{anode} - V_{electrolyte} - \Delta E^0$
Cathode/electrolyte interfaces	Potential continuity: $V_{cathode} = V_{electrolyte}$	Butler-Volmer kinetics: $\vec{j}.\vec{n} = i_{0,C}(e^{\frac{0,5F}{RT}\eta_C} - e^{-\frac{0,5F}{RT}\eta_C})$ with $\eta_C = V_{cathode} - V_{electrolyte}$

Table 2. Values of the model parameters

Parameter	**Description**	**Value**
j_{app}	Prescribed normal current density	3.54 x10^5 A.m^{-2} for a total prescribed current of 1000 A
ΔE^0	Equilibrium voltage (= $E^0_A - E^0_C$)	1.7 V
$i_{0,A}$	Exchange current density of the anodic reaction	0.001 A.cm^{-2}
$i_{0,C}$	Exchange current density of the cathodic reaction	1 A.cm^{-2}

2.3. Implementation in Comsol and meshing

Predefined physics interfaces are available in Comsol modules dedicated to electrochemistry, such as the Electrochemistry Module, for simulating current distributions in electrochemical devices. However, we chose here to use the *Electrostatics* physics interface, which is sufficient for simulating the present physics and which is available by default in the Comsol Multiphysics core. Three *Electric Current* physics are defined, one for each domain (anode, cathode, and electrolyte).

The domains are meshed using tetrahedral elements (figure 3). There is no need for a special level of refinement. However, it is important to ensure that there are enough elements on top of the anode, where the current is injected, as well as on the electrode edges, where current peaks are expected (edge effect). The total number of element approaches 66,000.

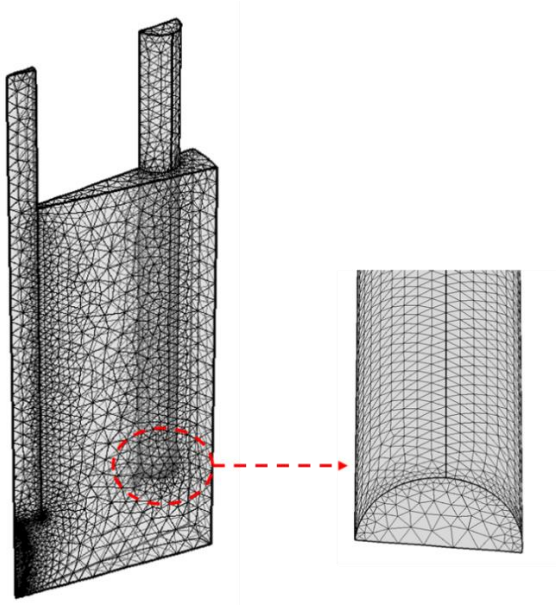

Figure 3. Meshing of the computational domains and detail of the elements on the anode/electrolyte boundary.

3. Results

The normal current density simulated at the electrode surfaces are shown on figure 4 for both current models and a total prescribed current of 1000 A. It is directly proportional to the local rate of the reactions.

In both current approaches, it is observed that the gas evolution reactions on the anodes are mainly concentrated on the inner parts facing the cathode. The deposition rate is quite uniform along the cathode height, with a significant current peak appearing around the bottom edge. The main difference between the primary and secondary descriptions is the uniformity of the current associated with the anodic reaction.

In the case of a primary distribution, the current density ranges from 0 to nearly 8 A/cm². In the secondary distribution, the anodic current density range is twice smaller, with a maximum value at 3.63 A/cm². This is due to the homogenization effect induced by the activation overpotentials, which are accounted for in the secondary model. The difference between the primary and secondary currents is much more attenuated at the cathode, where a similar level of heterogeneity is observed, due to the high value of the exchange current density $i_{0,C}$ considered in the secondary model for the cathodic reaction (see table 2).

The potential variations simulated across the cell for the two current models are represented in figure 5. The cell voltage can be decomposed into several contributions as shown in table 3. In the primary current model, the cell voltage (8 V) is the sum of the thermodynamic voltage ΔE^0 (1.7 V) and the Ohmic drops arising across the cell (6.3 V). In the secondary model, there is an additional activation term of 2.1 V due to the electrode kinetics, which brings the cell voltage up to 10 V. It can be noticed that, even though the average current density is much higher at the cathode due to its limited surface area, the reaction overpotentials is approximately 3-time higher (1.5 V compared to 0.6 V at the cathode) at the anodes whose reaction are very slow. For the two current models, the main contribution to the overall voltage are the Ohmic drops in the electrolyte.

Table 3. Details of the cell voltage contributions in both current approaches.

Current model	Decomposition voltage (V)	Ohmic drops (V)	Activation overpotentials η (V)	Overall cell voltage (V)
Primary distribution	1.7	6.3	0	8
Secondary distribution	1.7	6.5	1.5 (anodic) + 0.6 (cathodic)	10.3

The conclusion of the previous analysis is that the choice of a current model for predicting the reaction rate distribution and the voltage of an electrolysis cell will have a strong impact on simulations. Since most of the electro-refining processes involve at least one (kinetically slow) gas evolution reaction at the anodes, the secondary current approach is clearly more appropriate for such processes. By accounting for the reaction overpotentials, it will be more accurate than the primary approach in terms of current and voltage. Such electrical models can be used in order to optimize the cell design (number of electrodes and their arrangement into the cell) as well as the operating current, keeping in mind that the more homogeneous the reaction rate distribution is and the better the overall

performance of the cell will be. To illustrate the influence of the operating current on the reaction rate heterogeneity, figure 6 shows the deviation of the local secondary current density from its average value (ratio $j/j_{average}$) for three different total currents (500, 1000 and 2000 A). A clear trend to a more heterogeneous distribution is noticed when increasing the prescribed current, especially at the anodes. At the central cathode, the reaction rate is increased only at the very bottom edge while it remains quite stable on most of its surface. The values of the minimum and maximum simulated deviations are summarized in table 4.

Table 4. Minimum and maximum current deviation from the average value at each electrode, for the three current distributions presented in fig. 6.

Total current (A)	Current deviations at the anodes	Current deviations at the cathode
500	Min. 0.42 Max. 2.39	Min. 0.94 Max. 2.7
1000	Min. 0.28 Max. 3.4	Min. 0.91 Max. 3.6
2000	Min. 0.18 Max. 4.9	Min. 0.91 Max. 4.9

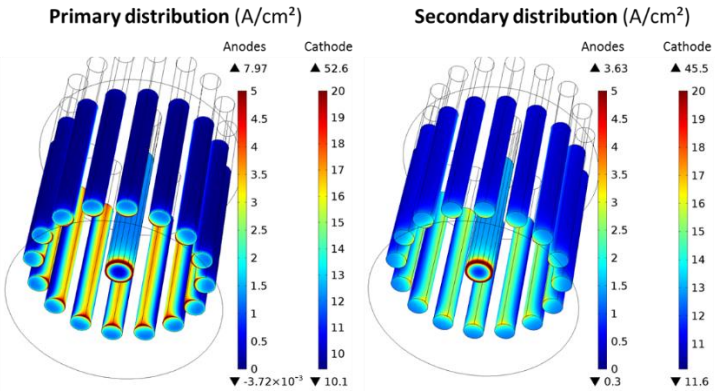

Figure 4. Current densities simulated at the electrode surface in the primary and secondary current models. Total current applied: 1000 A.

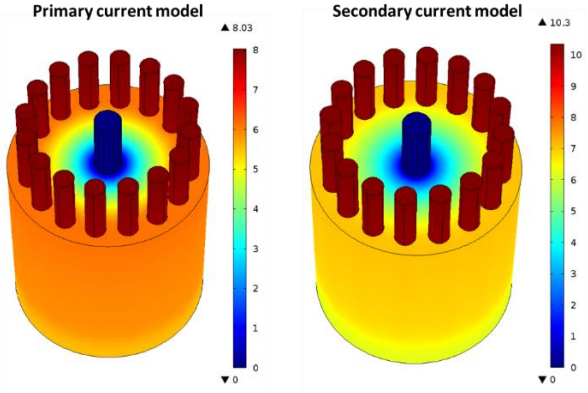

Figure 5. Potential distribution (V) throughout the electro-refining cell. Total current applied: 1000 A.

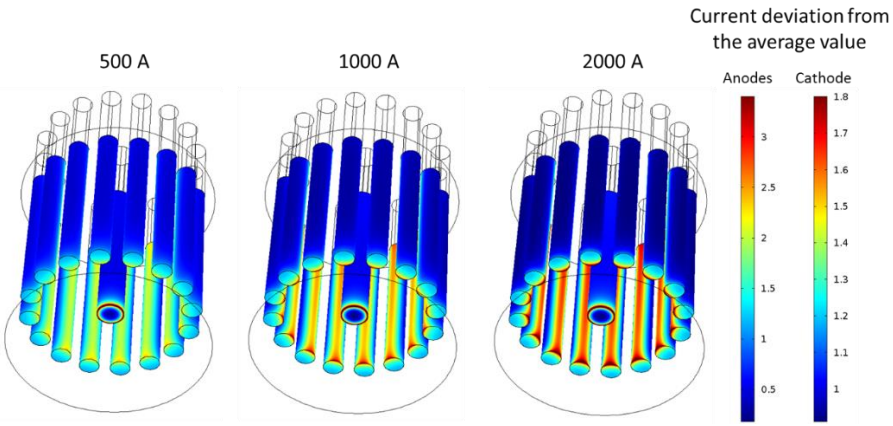

Figure 6. Deviation of the local current density from the average value at the electrode, for three different total currents prescribed to the cell.

4. Conclusion

In this study, we developed two didactic current models with COMSOL Multiphysics for simulating the reaction rate distribution in a typical molten salt electrolysis cell. The primary current model considers the reactions to be infinitely fast, while the secondary current model includes kinetics relations at the electrode/electrolyte interface. The results differ in terms of current uniformity (more uniform distributions for the secondary distribution) as well as cell voltage (significant contribution of the activation overpotentials in the secondary model). For such cells, a secondary approach is clearly more appropriate. The hetegeneization of the reaction rate distribution when increasing the prescribed current have been highlighted. These two models do not take into consideration the potential effect of the active species concentrations, which can arise at high current solicitation; such considerations can be envisaged with a more complex tertiary current model.

Acknowledgments: SIMTEC would like to thank the European Commission and the FP7 project REEcover (Project ID: 603564).